ELSEVIER

Journal of Alloys and Compounds 224 (1995) 111–116

Journal of ALLOYS AND COMPOUNDS

Electrical resistivity of metastable phases of $BaSi_2$ synthesized under high pressure and high temperature

Motoharu Imai, Toshiyuki Hirano

National Research Institute for Metals, 1-2-1, Sengen, Tsukuba, Ibaraki 305, Japan

Received 22 September 1994; in final form 6 December 1994

Abstract

Two metastable phases of $BaSi_2$, cubic $BaSi_2$ and trigonal $BaSi_2$, were synthesized under high-pressure and high-temperature conditions. The electrical resistivity and the dominant carrier of these two phases and the normal phase, orthorhombic $BaSi_2$, were measured at atmospheric pressure and temperature from 80 to 290 K. The electrical properties depend on the crystal structure. The orthorhombic $BaSi_2$ is an n-type semiconductor as previously reported. It is found that the cubic $BaSi_2$ is an n-type semiconductor and that the trigonal $BaSi_2$ is a hole metal. The change in the electrical properties with the structural change is discussed in terms of the change in the interatomic distances.

Keywords: Electrical resistivity; Metastable phase; High pressure; Barium silicide

1. Introduction

It is known that $BaSi_2$ has three phases at atmospheric pressure and room temperature. The first has an orthorhombic structure (the $BaSi_2$-type structure, Space group D_{16}^{2h}–*Pnma*), which is a stable form of $BaSi_2$ at atmospheric pressure and room temperature [1,2]. The second has a cubic structure (the $SrSi_2$-type structure [2,3], Space group O^6–$P4_332$) [4]. The cubic $BaSi_2$ is obtained by subjecting the orthorhombic $BaSi_2$ to the high-pressure and high-temperature conditions of 4 GPa and 600 to 800 °C [4]. The last has a trigonal structure (the $EuGe_2$-type structure [5], Space group D_3^{3d}–$P\bar{3}m1$) [6]. The trigonal $BaSi_2$ is obtained by subjecting the orthorhombic $BaSi_2$ to the high-pressure and high-temperature conditions of 4 GPa and 1000 °C [6]. The latter two phases are metastable at atmospheric pressure and room temperature. Each phase of $BaSi_2$ has a unique Si atom configuration as shown in Fig. 1. In the orthorhombic phase, the four Si atoms form tetrahedrons and each tetrahedron is separated from the other one by Ba atoms. The cubic phase has a three dimensional Si network. The trigonal phase has nearly two dimensional Si hexagonal layers. The layers are similar to those observed when one sees the elemental Si with the diamond-type structure from the [111] direction [7]. It is interesting to investigate the electronic properties in terms of the different Si atom configurations. At present, the orthorhombic phase is known to be a semiconductor with an energy gap of 1.3 eV [8] and no electronic properties of both the cubic and the trigonal phases have been investigated. In the present study, we synthesized the cubic and the trigonal phases of $BaSi_2$ and examined the electrical properties in the temperature range from 80 to 290 K for the cubic phase and 7 to 290 K for the trigonal phase.

2. Experimental

The starting material was the orthorhombic $BaSi_2$ with purity of 98% (obtained from Cerac Co.). The orthorhombic phase sample for the electrical measurements was fabricated by melting the starting sample in an argon arc furnace. The synthesis of the metastable phases was carried out using a modified belt-type apparatus at the National Institute for Research in Inorganic Materials [9]. The sample assembly is shown in Fig. 2. The cubic phase was synthesized according to the following procedure, referring to the previous work by Evers et al. [4]. First, the starting powder sample was compressed to 4 GPa at room temperature and heated up to 700 °C. After being maintained in this condition for 15 min, the temperature was lowered rapidly to room temperature by shutting off the supplied

SSDI 0925-8388(95)01530-2

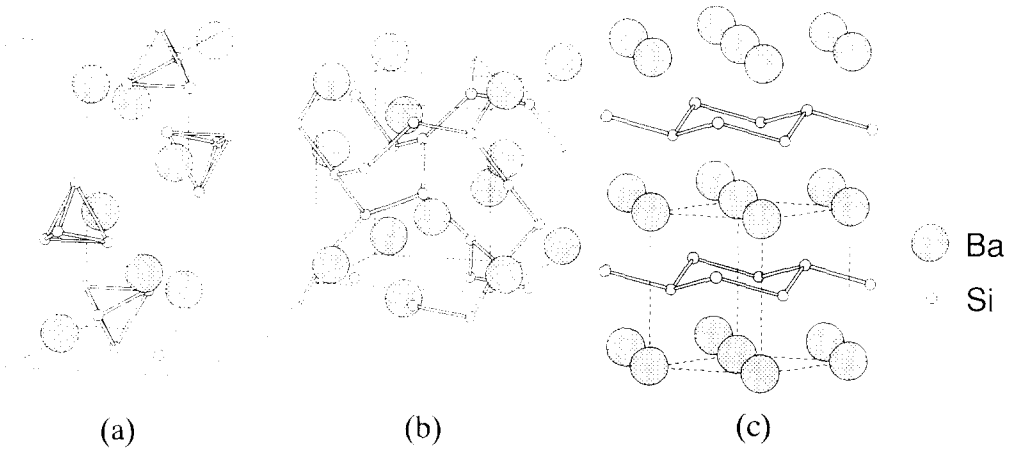

Fig. 1. The crystal structure of three polymorphs of $BaSi_2$. (a) The orthorhombic form, (b) the cubic form and (c) the trigonal form.

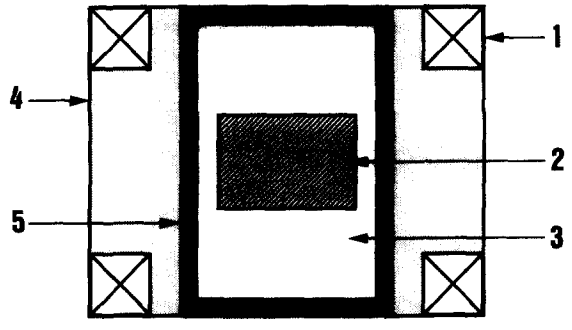

Fig. 2. Sample assembly for the high-pressure synthesis of metastable phases of $BaSi_2$: 1, steel ring; 2, sample (the orthorhombic $BaSi_2$); 3, hexagonal BN capsule; 4, NaCl–10 wt.% ZrO_2 pressure medium; and 5, graphite heater.

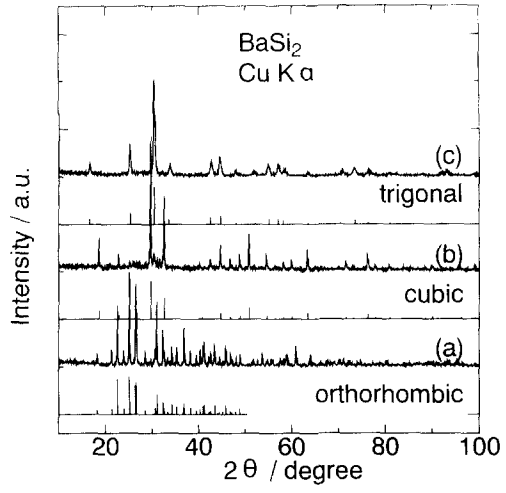

Fig. 3. X-ray diffraction patterns for (a) the orthorhombic phase, (b) the cubic phase and (c) the trigonal phase. The patterns shown by vertical bars are the simulated diffraction patterns.

electric power and finally the pressure was reduced. The trigonal phase was synthesized at 400 °C and 5.5 GPa for 120 min using the same procedure as for the cubic phase. The crystal structure of the synthesized samples was confirmed by X-ray diffraction measurement.

The electrical resistivity of the orthorhombic and trigonal $BaSi_2$ was measured using a conventional 4-probe method. Typical sample dimension was $7.0 \times 1.8 \times 0.5$ mm^2. For the cubic $BaSi_2$, the van der Pauw 4-probe method [10] was used because the sample was brittle. The thickness of the cubic sample was 0.31 mm. Spark-bonding of thin Au wires [11] was used for the electrical measurements of the trigonal $BaSi_2$, while bonding with a silver epoxy was used for the orthorhombic and the cubic samples because of their high electrical resistivity. The type of predominant carrier was determined thermoelectrically using a hot probe arrangement at room temperature [12].

3. Results and discussion

Fig. 3 shows the observed X-ray diffraction patterns of the three phases with their simulated patterns, which agree well with the results of Evers et al. [4,6]. Since no major extra peak is observed, the synthesized sample can be considered to be almost a single phase. The lattice parameters obtained are: $a = 8.91$ Å, $b = 6.72$ Å and $c = 11.53$ Å for the orthorhombic phase; $a = 6.72$ Å for the cubic phase; $a = 4.06$ Å and $c = 5.28$ Å for the trigonal phase (the parameters here are those of the equivalent hexagonal cell).

Fig. 4 shows the electrical resistivity of the three phases as a function of temperature. It should be noted that the resistivity and the temperature dependence of it strongly depend on the crystal structure. The resistivity decreases remarkably as the structure changes from the orthorhombic phase into the trigonal phase through the cubic phase. The orthorhombic phase shows the highest resistivity among the three phases and a large negative temperature dependence. The cubic phase also shows a negative temperature dependence but the resistivity is considerably lower than that of the or-

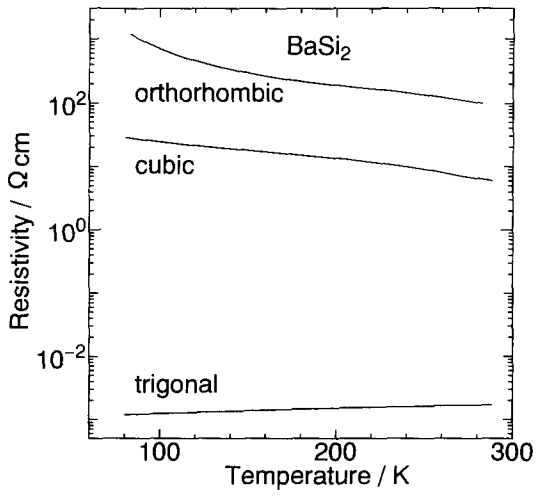

Fig. 4. Electrical resistivities of the orthorhombic, the cubic and the trigonal phases as a function of temperature.

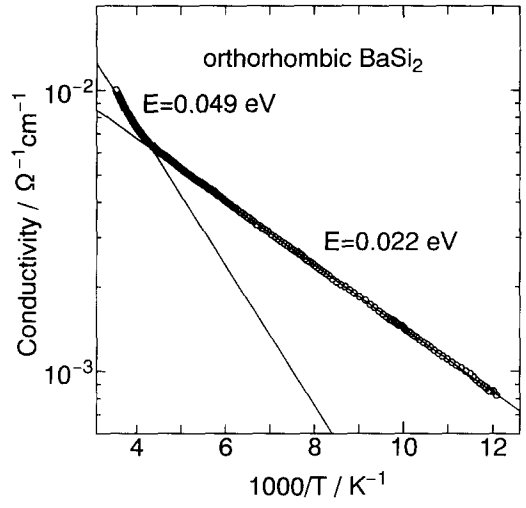

Fig. 5. Electrical conductivity of the orthorhombic phase as a function of reciprocal temperature, $1/T$. The solid lines are fitted lines to the following equation, $\sigma=\sigma_0\exp(-E/kT)$ with $E=0.049$ and 0.022 eV, respectively.

thorhombic phase. Meanwhile, the trigonal phase shows the lowest resistivity and a positive temperature dependence different from the other forms. The details will be described below.

As shown in Fig. 4, the resistivity of the orthorhombic phase showed a negative temperature dependence like a semiconductor. Fig. 5 shows a semi-logarithmic plot of the conductivity, σ, as a function of reciprocal temperature, $1/T$. The conductivity can be well fitted to two linear relations against $1/T$, indicating that the electrical conduction is controlled by a thermally activated mechanism in both the higher and lower temperature regions. From thermoelectric data, the dominant carriers are electrons. Thus, the orthorhombic $BaSi_2$ is an n-type semiconductor, which is consistent with the results by Evers and Weiss [8]. Small activation energy of 0.049 eV was obtained for the higher temperature range above 230 K. Evers and Weiss reported 1.3 eV for the energy gap in the temperature range from 293 to 1073 K [8]. According to their data, the activation energy is expected to be 0.65 eV, since the activation energy in the intrinsic region is about a half of the energy gap. Probably the small activation energy in the present study is attributed to the temperature range used, which is too low to measure the exact activation energy of the intrinsic range. Since the sample is not free from impurities and defects, this small activation energy may correspond to the energy gap between the conduction band edge and the donor level due to the impurities, defects or a combination thereof.

The resistivity of the cubic phase also exhibited a negative temperature dependence with increasing temperature in the same way as that of the orthorhombic phase. But the conductivity, σ, cannot be fitted to the log σ-T^{-1} as shown in Fig. 6, though the reason is not clear. However, taking account of the large resistivity, 5.6 Ωcm at room temperature, and the negative temperature dependence, this phase may be a semiconductor. Since the dominant carriers are electrons, the cubic $BaSi_2$ may be an n-type semiconductor as well as the orthorhombic phase. The semiconducting behavior of the cubic $BaSi_2$ is different from the metallic behavior of the other alkaline-earth metal disilicide, $SrSi_2$ [8], which has the same structure as the cubic $BaSi_2$.

Different from the former two phases, the trigonal phase showed a positive temperature dependence of the resistivity and the predominant carriers are holes. Fig. 7 shows the resistivity, ρ, of the trigonal $BaSi_2$ as a function of temperature. Matthiessen's rule holds for the resistivity, i.e. it is expressed by the sum of the residual resistivity and the thermal component. The residual resistivity is very large, 1.1×10^3 μΩcm at 8 K, which implies that many lattice defects exist in the

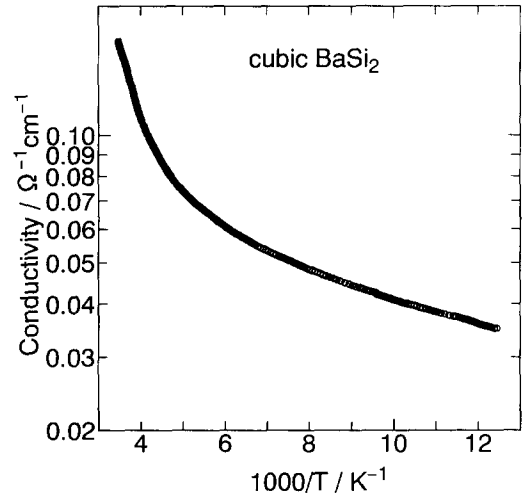

Fig. 6. Electrical conductivity of the cubic phase as a function of reciprocal temperature, $1/T$.

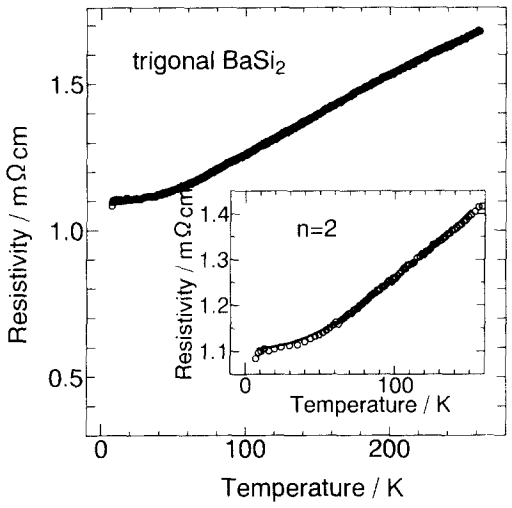

Fig. 7. Temperature dependence of the electrical resistivity of the trigonal phase. The solid line in the inset represents the fitted curve to the equations in the text. The fitted parameters are: $n=2$, $\rho_0=1.11\times10^3$ μΩcm, $A=1.77\times10^3$ μΩcm and $\Theta_D=611$ K.

sample. In spite of the large residual resistivity, the trigonal phase showed a marked positive temperature dependence of the resistivity. The results indicate that the trigonal $BaSi_2$ is a metal. The resistivity data are analyzed in more detail using Matthiessen's rule and Bloch–Grüneisen equation, i.e. by the sum of residual resistivity ρ_0 and the thermal component $\rho_{th}(T)$as follows:

$$\rho(T)=\rho_0+\rho_{th}(T)$$

$$\rho_{th}(T)=A(T/\Theta_D)^n\int_0^{T/\Theta_D}\frac{z^n\,dz}{(e^z-1)(1-e^{-z})}$$

where Θ_D is the Debye temperature and A and n are constants. The parameters ρ_0, Θ_D and A are evaluated by minimizing the residual square sum (RSS) by a non-linear least squares method [13,14]. The value of RSS is given by the following equation

$$\mathrm{RSS}=\sum_{i=1}^{N}[\rho_i(T)_{\mathrm{meas}}-\rho_i(T)_{\mathrm{calc}}]^2$$

where N is the number of the points and $\rho_i(T)_{\mathrm{meas}}$ and $\rho_i(T)_{\mathrm{calc}}$ are the measured and calculated resistivities, respectively. Since the negative deviations from the Bloch–Grüneisen relation was observed above 150 K, the analysis was carried out for the data below 150 K. The best fit is obtained when the exponent n is 2 as shown in the inset of Fig. 7. The fitted parameters are: $n=2$, $\rho_0=1.11\times10^3$ μΩcm, $A=1.77\times10^3$ μΩcm and $\Theta_D=611$ K. However, it is now difficult to specify a scattering mechanism for the $n=2$ exponent because the exponent has a clear physical meaning for 3 and 5 [15–17].

Table 1 compares the present results with the results with $CaSi_2$ [14]. $CaSi_2$ has almost the same structure as the trigonal $BaSi_2$ except for a slight difference in the stacking sequence of the metal layers and the hexagonal Si layers. The residual resistivity is much larger than that of $CaSi_2$ and as a result, the residual resistivity ratio is small. In spite of the large residual resistivity, the temperature coefficient of resistivity, $\Delta\rho/\Delta T$, is also much larger than that of $CaSi_2$.

Pressure-induced semiconductor–metal transition is reported in many semiconductors such as Si, GaAs [18], Se [19] and so on. Most of the metallic high-pressure phases are, however, not stable and return immediately to the semiconductive phase when pressure is released. As far as we know, it is rarely known that the pressure-induced metallic phase can exist at atmospheric pressure and room temperature as a metastable phase.

The electrical properties varied drastically with the structural change. As mentioned in Section 1, the most striking structural feature of the three $BaSi_2$ polymorphs is the unique Si atom configurations, i.e. tetrahedra in the orthorhombic phase, three dimensional network in the cubic phase, and nearly two dimensional network in the trigonal phase. We consider that the structural change of the $BaSi_2$ with the different Si configurations is related to the interatomic distance variation, especially the decrease of the Ba–Ba and Ba–Si distances, as follows. Table 2 lists the interatomic distances and coordination numbers of the three polymorphs of $BaSi_2$. Table 3 compares the interatomic distances of the Ba–Ba, Ba–Si and Si–Si in the three phase. It should be noted that the Ba–Ba and Ba–Si distances decrease with the structural change. On the other hand, the Si–Si distance of the three phases, which is slightly longer than that of diamond-type structure Si (2.35 Å), is almost unchanged. The easier reduction of the Ba–Ba distance than the Si–Si distance is reasonable from the fact that the bulk modulus of bcc Ba (8.93 GPa) [20] is much smaller than that of the crystalline Si (97.88 GPa) [21]. Probably the easier reduction of the Ba–Ba and Ba–Si distances causes the structural change, resulting in the different Si networks. We also consider that in $BaSi_2$, the electronic structure near the Fermi level is due to the interaction between the Ba atoms and Si atoms in the networks, which is reflected in the electrical properties.

So far, the electronic structures of $BaSi_2$ have never been calculated and it is impossible to discuss them strictly. However, Fahy and Hamann [22] calculated the electronic structure of $CaSi_2$, whose structure is the same as that of the trigonal $BaSi_2$. They pointed out that the interaction between the Ca layers and the dangling bonds of the Si hexagonal layers plays a critical role in the electronic structures near the Fermi level. The 3d states of the Ca atoms hybridize strongly with the dangling-bond states of the Si hexagonal layers and the hybridized state crosses the Fermi level, which

Table 1
Summary of the resistivity measurement of the trigonal $BaSi_2$, compared with the data of the $CaSi_2$ [14]

Sample	Resistivity ($\mu\Omega$cm) 8 K	273 K	Residual resistivity ratio ρ(273 K)/ρ(8 K)	Temperature coefficient $\Delta\rho/\Delta T$ ($\mu\Omega$c m/K)
Trigonal $BaSi_2$	1.10×10^3	1.71×10^3	1.6	2.3
$CaSi_2$[110]	19.5	63	3.2	0.16
[111]	25.4	56	2.2	0.12

Table 2
Interatomic distances (in Å) and coordination numbers for $BaSi_2$
The number before the atomic symbole represents the coordination number. The number in the parentheses represents the kind of atom site

Orthorhombic $BaSi_2$									
Ba(1)		Ba(2)		Si(1)		Si(2)		Si(3)	
2Ba(1)	4.64	2Ba(1)	4.25	1Si(2)	2.41	1Si(1)	2.41	1Si(1)	2.47
2Ba(2)	4.25	1Ba(1)	4.75	2Si(3)	2.47	2Si(3)	2.37	1Si(2)	2.37
1Ba(2)	4.75	1Ba(1)	4.76	1Ba(1)	3.39	1Ba(1)	3.34	1Si(3)	2.32
1Ba(2)	4.76	2Ba(2)	4.46	2Ba(1)	3.62	1Ba(1)	3.61	1Ba(1)	3.41
1Si(1)	3.39	1Si(1)	3.64	1Ba(2)	3.64	1Ba(2)	3.14	1Ba(1)	3.49
2Si(2)	3.62	1Si(2)	3.14			2Ba(2)	3.56	1Ba(2)	2.95
1Si(2)	3.34	2Si(2)	3.56					1Ba(2)	3.65
1Si(2)	3.61	2Si(3)	2.95					1Ba(2)	3.68
2Si(3)	3.42	2Si(3)	3.65						
2Si(3)	3.49	2Si(3)	3.68						
Cubic $BaSi_2$									
Ba		Si							
6Ba	4.11	3Si	2.45						
6Si	3.37	3Ba	3.37						
2Si	3.42	1Ba	3.42						
Trigonal $BaSi_2$									
Ba		Si							
6Ba	4.05	3Si	2.45						
6Si	3.28	3Ba	3.28						

Table 3
The interatomic distances in the three phases of $BaSi_2$
The numbers in the parentheses are average interatomic distances calculated taking account of the coordination number

	Ba–Ba	Ba–Si	Si–Si
Orthorhombic $BaSi_2$	4.25–4.76 (ave. 4.52)	2.95–3.68 (ave. 3.47)	2.32–2.47 (ave. 2.40)
Cubic $BaSi_2$	4.11	3.37	2.45
Trigonal $BaSi_2$	4.05	3.28	2.45

makes $CaSi_2$ metallic. Probably the same story can be applied to the trigonal $BaSi_2$, i.e. the electronic structure near the Fermi level is attributed to the hybridized states of the 5d states of Ba atoms and the dangling bond states of the Si networks, which makes the trigonal $BaSi_2$ metallic.

4. Conclusion

The results are summarized as follows. (1) The cubic and trigonal phases of $BaSi_2$ were synthesized using the belt-type apparatus, (2) the resistivity and its temperature dependence changed drastically with the structural change, (3) the cubic $BaSi_2$ is an n-type semiconductor, (4) the trigonal $BaSi_2$ is a hole metal, and (5) the electrical properties with the structural change can be considered to be ascribed to the Ba–Ba and Ba–Si distances.

Acknowledgments

The authors would like to thank Drs. T. Taniguchi and S. Yamaoka of the National Institute for Research

in Inorganic Materials for their help in high-pressure synthesis. We are also grateful to Dr. T. Hatano for his technical advise in the low temperature measurements, Dr. N. Kishimoto for his useful discussion and Dr. Furubayashi for critical reading of the manuscript.

References

[1] H. Schäfer, K.H. Janzon and A. Weiss, *Angew. Chem. Int. Ed. Engl., 2* (1963) 393.
[2] K.H. Janzon, H. Schäfer and A. Weiss, *Z. Anorg. Allg. Chem., 372* (1970) 87.
[3] K.H. Janzon, H. Schäfer and A. Weiss, *Angew. Chem. Int. Ed. Engl., 4* (1965) 245.
[4] J. Evers, G. Oehlinger and A. Weiss, *Angew. Chem. Int. Ed. Engl., 17* (1978) 538.
[5] E.I. Gladyshevskii, *Dopov. Akad. Nauk. Ukr. RSR, 2* (1964) 209.
[6] J. Evers, G. Oehlinger and A. Weiss, *Angew. Chem. Int. Ed. Engl., 16* (1977) 659.
[7] A.F. Wells, in *Structural Inorganic Chemistry*, Clarendon, Oxford, 1984, 5th edn., p. 130.
[8] J. Evers and A. Weiss, *Mat. Res. Bull., 9* (1974) 549.
[9] S. Yamaoka, M. Akaishi, H. Kanda, T. Osawa, T. Taniguchi, H. Sei and O. Fukunaga, *J. High Pressure Inst. Jpn., 30* (1992) 249.
[10] L.J. van der Pauw, *Philips Res. Rep., 13* (1958) 1.
[11] Iye, T. Tamegai, H. Takehaya and H. Takei, *Jpn. J. Appl. Phys., 27* (1988) L658.
[12] K. Seeger, in *Semiconductor Physics*, Springer-Verlag, Berlin, 1991, 5th edn., p. 83.
[13] T. Hirano and M. Kaise, *J. Appl. Phys., 68* (1990) 627.
[14] T. Hirano, *J. Less-Common Met., 167* (1991) 329.
[15] N.F. Mott and H. Jones, in *The Theory of the Properties of Metals and Alloys*, Dover, New York, 1958.
[16] G.W. Webb, *Phys. Rev., 181* (1969) 1127.
[17] F.J. Pinski, P.B. Allen and W.H. Butler, *Phys. Rev., B23* (1981) 5080.
[18] S. Minomura and H.G. Drickamer, *J. Phys. Chem. Solids, 23* (1962) 451.
[19] F.P. Bundy and K.J. Dunn, *J. Chem. Phys., 71* (1979) 1550.
[20] M.S. Anderson, C.A. Swenson and D.T. Peterson, *Phys. Rev., B41* (1990) 3329.
[21] *Crystal and Solid State Physics*, Vol. I of Landolt–Börnstein, *Numerical and Functional Relationships in Science and Technology*, Springer-Verlag, Berlin, 1966.
[22] S. Fahy and D.R. Hamann, *Phys. Rev., B41* (1990) 7587.